Journal of Advanced Zoology

ISSN: 0253-7214

*Volume **43** Issue **1 Year 2022** Page **368:386***

Formulation, Optimization and Evaluation of Nano Based Novel Ophthalmic Drug Delivery System for Glaucoma

Monali Dumore[1*], Praveen Sharma[2], Sachin Kumar Jain[3], Sudha Vengurlekar[4], Nitin Dumore[5]

[1,2,3,4]Department of Pharmacy, Oriental University, Indore, M.P*
[5]Department of Pharmacology, Dadasaheb Balpande College of Pharmacy, Nagpur, M.H

***Corresponding author:** Monali Dumore*
**Department of Pharmacy, Oriental University, Indore, M.P*

Abstract

Drugs delivered topically using traditional administration methods have a low bioavailability. Therefore, the goal of the current study was to create and refine the in-situ gel of carteolol-loaded chitosan nanoparticles (CHNPs), which were made using the ionotropic gelation method. Using formulation variables such as CH (A), STPP concentration (B), and stirring speed (C), the formulation was optimised by the application of box-Behnken design. Their impacts on the independent variables, such as entrapment efficiency (Y2) and particle size (Y1), were assessed. Additionally, the physicochemical properties, in-vitro drug release, ex-vivo permeability, bioadhesive studies, corneal hydration, histopathology, and HET-CAM of Carteolol-CHNPs were assessed. Nanoparticles loaded in-situ gel were also analysed. The tiny particle size (153 ± 6 nm) of the optimised formulation (Carteolol-CHNP opt) is ideal for ocular administration. In addition, it had a spherical form, a high encapsulation rate (71.06%), and a positive zeta potential (+36.3 mV). A sustained drug release profile (83.99 ± 3.6% over 12 hours) was found in the drug release research. Hydration, histology, and the HET-CAM test all reveal that the excised goat cornea in the CHNPs loaded in-situ gel did not show any signs of injury. The outcomes shown that glaucoma patients with a longer precorneal residency length and better patient compliance could benefit from the use of Carteolol-CHNPs loaded in-situ gel by reducing the dosage frequency.

Keywords: Glaucoma, Ophthalmic, Nanoparticles, Chitosan, In-situ gel, Novel, etc.

Introduction

The most popular and easily accessible location for topical medication delivery is the eye. The medications can be injected into the eye area to have both a local and systemic effect. Due to their intricate anatomy and physiology, the eyes have proven to be difficult targets for medication administration. Glaucoma is a dangerous condition of the eyes that is defined by elevated intraocular pressure. It causes no symptoms at first and eventually impairs vision by damaging the optic nerve. Unbalance between the ocular chamber's

drainage mechanisms and aqueous humour secretion may lead to the development of glaucoma [1,2]. Many medications are available to treat these diseases; the most popular dosage form is eye drops. Eye drops are widely accepted for use by glaucoma patients due to their affordable cost, simplicity of production, patient compatibility, and tolerability [3,4]. Nevertheless, there are significant issues with those eye drops, including quick precorneal drainage, low permeability, short residence time, and poor absorption [5]. Furthermore, increased concentrations of certain medications may irritate and sting the eyes [6].

The primary objective of glaucoma treatment is the development of an alternate method for delivering glaucoma medications. Long-acting ocular drug delivery systems are required for greater patient compliance, enhanced local bioavailability, decreased dose concentration, and dosing frequency due to several drawbacks with standard eye drops. It is thought that some of the issues with traditional eye drops can be resolved by using an in-situ gel medication delivery system. When compared to conventional drug delivery systems, in situ gel ophthalmic drug delivery systems have several advantages, including sustained extended action, simpler production procedures, and lower manufacturing costs [7, 8]. In situ gel systems are made up of stimuli-responsive or smart polymers that, in response to changes in temperature, pH in the precorneal region, or the electrolyte content of the tear film, display sol to gel phase transitions in the eye [9–11].

In general, polyelectrolytes with basic or acidic groups in their structure that can absorb or release protons in reaction to pH variations in their surroundings are known as pH-sensitive polymers [12]. For the preparation of pH-triggered gels, carbopol is frequently utilised in ocular formulations [13–15]. In the solid state, the carbopol molecule frequently takes the shape of a highly coiled spiral; hydration of this spiral form increases viscosity [16]. Excellent organoleptic properties, gel formation at low concentrations, stability, and compatibility with a wide range of active ingredients are all features of carbopol [17].

To improve medication retention and penetration, a variety of polymeric nano-formulations have been investigated. Because they are non-toxic and biodegradable, these are widely accepted. Ocular polymeric nanoparticles are made of a variety of polymers, including chitosan, galactomannan, eudragit RS-100, sodium alginate, pectin, and tamarind kernel polysaccharide. Of these, chitosan (CH) is the most well-known and widely utilised polymer in various ocular delivery systems. It is a naturally occurring cationic polysaccharide polymer that is produced when chitin is deacetylated. Furthermore, CH has a potent bioadhesive quality that delays its quick removal from the ocular area by lengthening the corneal contact period. In comparison to a traditional viscolizer, the formulation made with CH produces less viscosity. It becomes protonated (NH_3^+) in acidic media and is soluble in it. The primary benefit is that CH has a positive charge at physiological pH. It interacts with mucin's negative charge to improve bioadhesion [18,19]. A frequent treatment for glaucoma is the nonselective β-adrenergic receptor blocking drug carteolol. It hasn't, however, yet been released on the market as an ocular in situ gel [20].
agent and commonly used in the treatment of glaucoma (Chrisp and Sokin 1992). However, it has not been marketed as an ocular in situ gel yet.

The current study's goal was to create CHNPs loaded with carteolol using the ionotropic gelation technique. Three factors at two levels were used to optimise the formulation. Additionally, in-vitro drug release, solid-state characterisation, and the formulation and investigation of the impact of polymer composites on produced nanoparticles loaded in situ gel were also conducted using the optimised Carteolol-laden CHNPs formulation.

Material and Method

Materials

Chitosan (MW 120,000, deacetylation degree 85%) was gifted from Indian Sea Food (Kochi, India) that is made from crab shell. SD Fine Chemical (Mumbai, India) provided the sodium tripolyphosphate (STPP). We bought pig mucin from Himedia in Mumbai, India. Chemicals for the phosphate buffer and glacial acetic acid were purchased from Sigma Aldrich. Analytical grade compounds were all that were employed in the research.

Method of Preparation

Carteolol-CHNPs were formulated using the ionotropic gelation technique. Table 1 displays the composition of a total of 17 formulations that were selected in accordance with the BBD design. The aqueous glacial

acetic acid solution (1% v/v) was used to dissolve the various concentrations of CH (0.1–0.35%). The various STPP concentrations (0.1–0.4%) were separately dissolved in double-distilled water. Carteolol (25 mg) was measured out, dissolved in CH solution, and then gradually added to STPP solution while being constantly stirred (between 1000 and 2500 rpm). The produced NPs were separated using the ultracentrifugation method at 15,000 rpm (Remi 24, Cooling centrifuge, Mumbai, India). After that, they were cleaned with distilled water and lyophilized using mannitol (2% w/w) as a cryoprotectant (Thermo Electronic, Germany's Heto-powder dry LL1500 freeze drier). The lyophilized material was gathered and kept in storage to conduct additional analysis.

Table 1: Carteolol -Loaded Chitosan Nanoparticles Composition and Their Effect on Particle Size (Y1) and Entrapment Efficiency (Y2)

Formulation	Independent Variables			Responses			
	A – CH (%, w/v)	B – STPP (%, w/v)	C – Stirring Speed (rpm)	Particle Size (nm, Y1)		Entrapment Efficiency (%, Y2)	
				Actual Value	Predicted Value	Actual Value	Predicted Value
1	0.10	0.1	2500	116.80	116.56	41.13	41.08
2	0.35	0.1	2500	247.44	247.63	49.48	49.54
3	0.10	0.4	2500	111.43	111.23	71.34	71.28
4	0.35	0.4	2500	187.15	187.39	62.55	62.59
5	0.10	0.25	1000	172.93	173.38	58.17	58.16
6	0.35	0.25	1000	284.76	284.78	69.10	68.98
7	0.10	0.25	4000	117.81	117.78	48.44	48.55
8	0.35	0.25	4000	210.09	209.63	37.50	37.50
9	0.22	0.1	1000	203.35	203.13	55.61	55.66
10	0.22	0.4	1000	174.33	174.06	73.07	73.14
11	0.22	0.1	4000	139.22	139.48	31.03	30.96
12	0.22	0.4	4000	103.27	103.98	56.80	56.75
13	0.22	0.25	2500	155.13	155.11	52.99	53.31
14	0.22	0.25	2500	154.55	155.11	53.24	53.31
15	0.22	0.25	2500	156.31	155.11	53.66	53.31
16	0.22	0.25	2500	155.33	155.11	53.44	53.31
17	0.22	0.25	2500	154.27	155.11	53.25	53.31

Optimization

The formulation was optimized via Box-Behnken design utilizing software (Design Expert 7.0.0) in accordance with the preliminary study results. Three distinct levels—low (-), medium (0), and high (+)—were used to measure the independent variables CH (A), STPP concentration (B), and stirring speed (C). To compare the various models, the impact of independent factors on dependent variables was evaluated. To determine the impact of each answer, the independent variables [particle size (X1) and encapsulation efficiency (X2)] were examined. Table 1 illustrates the design, which included a total of 17 runs with five common formulas. To find the best fit model, the responses of several formulations were fitted into linear, 2nd order, and quadratic models. Three-dimensional surface plots and a polynomial equation were created to examine the impact of independent variables on dependent variables.

Characterization

Particle characterization

Using a zeta sizer (Malvern zeta sizer nano, Malvern UK), the produced Carteolol -CHNPs were assessed for size, polydispersibility index (PDI), and zeta potential (ZP). The sample (0.1 mL) was taken, diluted (100 times) using double distilled water, and then the assessment was carried out for the specified parameters. Transmission electron microscopy (JEM1011, JEOL, Inc., Peabody, MA, USA) was used to examine the morphology of the optimized nanoparticle (Carteolol -CHNP opt). After placing a drop of the sample on the copper-coated grid, 2% v/v phosphotungstic acid was administered to the formulation to act as a stain. After removing the surplus volume and letting it air dry, the sample was put in a position to assess the particle morphology.

Thermal Analysis

Carteolol, CH, and Carteolol -CHNP opt were subjected to thermal analysis using the DSC 6000 equipment (Perkin Elmer, Waltham, MA 02451, USA). Each sample was taken in an acceptable quantity (~ 5 mg) and sealed in a sample pan. The sealed samples were put within a DSC apparatus and continuously supplied with nitrogen as they were scanned at a pace of 5ºC/min between 0 and 300°C.

X-Ray Diffraction Study

The x-ray diffraction equipment (Philips PW 3710, Eindhoven, Netherlands) was used to analyses the diffractogram of Carteolol, CH, and CTM-CHNP opt to verify any changes in the sample's composition. The samples were put into the instrument after being filled into the sample holder. The test was run with a 35 kV voltage and a Cu-anode radiation source. At room temperature, the samples were scanned at a scanning rate of 1º between 5º and 70º (2 ɧ). Every spectra were captured and compared in order to assess the diffraction angle change.

In-vitro Release Study

Using a dialysis bag, the medication was released from the produced Carteolol -CHNP opt and Carteolol solution (control). A dialysis bag containing five milliliters of sample was filled and secured at both ends. The release medium, simulated tear fluid (STF), was added to the bag and swirled at 50 revolutions per minute. Fresh release medium was substituted for the released samples (2 mL) at prearranged intervals of 1, 2, 3, 4, 6, 8, and 12 hours. After the proper dilution, the released drug concentration was measured at each time point using a UV spectrophotometer (Shimadzu 1800 UV Spectrophotometer, Japan) at a particular wavelength. To verify the release mechanism, the in-vitro release data were fitted into various release kinetic models, such as the zero-order, first-order, Korsmeyer Peppas, Higuchi, and Hixon–Crowell models. The best-fit release kinetic model was chosen by utilizing the regression coefficient (R2) as a parameter.

FORMULATION OF NANOPARTICLE LOADED THERMOSENSITIVE *IN SITU* GEL

Weigh the polymer (HPMC) precisely in the ratios of 1%, 1.5%, and 2%. Heat the water to a fresh boil, let it cool, then combine the gelling agent (carbopol) with glycerine (as per the lubricating agent's triking plan) and a wetting agent in an equal amount in a glass mortar. Add the mixture to the benzalkonium chloride fluid, stirring until the mixture becomes transparent and uniform gels are formed.

Table 2: Formulation Contents of Nanoparticle Loaded Thermosensitive In-Situ Gel

Batch Name	Nanoparticles Concentration containing carteolol (gm)	HPMC
F1	0.25	1 %
F2	0.25	1.5 %
F3	0.25	2 %

Characterization of nanoparticles loaded in situ gel

Clarity and pH

Clarity is one of the important features of ophthalmic formulations. All prepared formulations were evaluated for clarity by visual observation against black and white background. Clarity of all formulations was found to be satisfactory.

The developed formulation should be non-irritant after administration. The developed formulations were evaluated for pH. The pH of all formulation was in the range of 6.4 to 6.8. Ocular site can tolerate pH in the range of 3.5 to 8.5 without sensitization to patient significantly. Results are shown in table no. 7.

Gelling capacity

Gelling capacity of all prepared batches was determined in simulated tear fluid at 37˚C. None of the batch failed to gel at physiological pH. However; batch F3 and F2 showed less stable gel (++) in comparison to F1 batch. This effect might be due to less concentration of polymer which failed to hold gel structure for longer duration. Results are depicted in table no. 8.

Viscosity

Viscosity is the most important parameter of ocular formulation that affects patient compliance as well as residence time of formulation. If it is very high then it results in patient discomfort and if it is very less, then it gets drain off from eye rapidly. At the same time, viscosity should be less in container, so that formulation can be easily administer.

Drug release

All batches of nanoparticle loaded *in situ* gel formulation were subjected for *in vitro* drug release study by using dialysis sac. The percent cumulative drug release for prepared batches at the end of 10 h. Results are shown in table no. 10.

Gelation temperature

Gelation temperature is one of the important property of temperature triggered *in situ* gel formulation. Conversion of sol form to gel form at or slightly below to physiological temperature is the prerequisite for these kind of system. The temperature at which this sol to gel transition takes place is known as gelation temperature. Fabricated batches of NPs loaded *in situ* gel was subjected for gelation temperature estimation. Results are shown in table no. 11.

Sterility testing

Sterility is one of the major requirements of ophthalmic preparations. Fabricated NPs loaded *in situ* gel was subjected for sterility testing as per Indian Pharmacopoeia 2010, to ensure that selected method is enough to make system sterilized. NPs were placed in UV chamber for 1.5 h and transferred aseptically in autoclaved *in situ* gel system. No turbidity was observed in test sample at the end of 14 days. On the other hand, significant turbidity was observed in positive control. Result supports the usefulness of selected method for sterilization. Results are shown in figure no. 8.

FORMULATION OF PH-TRIGGERED IN SITU GEL CONTAINING NANOPARTICLES

Firstly, the gel solutions will be prepared by dispersing required amount of carbopol in deionized water with continuous stirring until complete dissolution and the volume was finally made up using deionized water. The nanoparticles dispersed in sufficient amount of gelling solution to obtain final concentration.

Table 3: Formulation Contents of pH-Triggered in Situ Gel Containing Nanoparticles

Ingredient	F1	F2
Carteolol nanoparticles	0.25	0.25
Carbopol	0.5	0.5
Methocel E50 LV	1.5	1.5
Sodium hydroxide	0.16	0.16
Benzalkonium chloride	0.02	0.02
Tween 20	-	1.0
Citric acid	0.407	0.407
Disodium hydrogen phosphate	1.125	1.125
Purified water	100 ml	100 ml

Evaluation of formulations

Clarity by visual observation against a black and white background in a well-lit cabinet, pH.

In-vitro release studies

Using a modified USP XXIII dissolving testing device, the in vitro release of carteolol from the formulations was investigated through cellophane membrane. The artificial tear fluid (pH 7.4) was freshly manufactured and utilized as the dissolving medium. A glass cylinder with a 5 cm diameter that was specially made and open at both ends was fastened to one end with a cellophane membrane that had been immersed in the dissolving medium for the previous night. Precisely 1 millilitre of the mixture was pipetted into this assembly. The cylinder was fixed to the driveshaft made of metal and submerged in 50 milliliters of dissolution medium that was kept at 37 degrees Celsius, only allowing the membrane to lightly touch the surface of the receptor media. At 50 rpm, the shaft was turned. At hourly intervals, 1-ml aliquots were removed and replaced with an equivalent volume of the receptor media. UV spectrophotometry was used to analyses the aliquots after they had been diluted with the receptor media.

Ex-vivo Permeation Study

Goat corneas were used in the ex-vivo permeation research of pH-Triggered in Situ Gel Containing Nanoparticles and Carteolol -solution. All operations were carried out in an aseptic environment, and goat eyeballs were obtained from an abattoir and placed in a sterile beaker. Extra tissue was removed from the eyeballs after they had five Phosphate Buffer Saline (PBS) washes. The goat eye's cornea was removed, and it was then placed at 4˚C in normal saline (0.9% w/v). The removed cornea was positioned with its active surface area of 1.5 cm^2 between the diffusion cell's donor and acceptor compartments. STF was added to the acceptor compartment, and one millilitre of each sample was added to the donor compartment. The investigation was conducted at 50 rpm and 37 ± 0.5ºC. At predetermined intervals, the permeating aliquots

(1 mL) were removed and concurrently replaced with an equal volume of fresh STF. The previously approved RP-HPLC technique was used to quantify the permeated concentration of each sample.

Bioadhesion Study

Pig mucin was used to test the bioadhesive strength of pH-Triggered in Situ Gel Containing Nanoparticles. In STF, the pig mucin (0.05 M) suspension was made. Pig mucin (1 mL) was added to the placebo and pH-Triggered in Situ Gel Containing Nanoparticles, and the mixture was incubated for 30 minutes. Using a cooling centrifuge (4ºC, Remi-24, 15,000 rpm), the sample was ultracentrifuged. Using a UV-Vis-1800 spectrophotometer (Shimadzu, Tokyo, Japan), the clear supernatant was separated and the amount of free mucin was measured. The following formula was used to determine the mucoadhesive strength.

$$\% \text{ Bioadhesion strength} = \frac{\text{Initial conc of pig mucin - Conc of pig mucin in supernatant} \times 100}{\text{Initial conc of pig mucin}}$$

Corneal Hydration Study

To assess the hydration of the cornea following treatment with pH-Triggered in Situ Gel Containing Nanoparticles, a study on corneal hydration was conducted. The cornea was taken out of the diffusion cell once the corneal permeation investigation was finished. Wet weight refers to the weight that was measured for the cornea. The wet cornea was weighed, and then it was dried and placed in a hot air oven (Thermo Scientific, Germany) set at 60˚C for three days. The following formula was used to determine the corneal hydration.

$$\% \text{ Corneal hydration} = \frac{\text{Wet weight of cornea - Dry weight of cornea} \times 100}{\text{Dry weight of cornea}}$$

Histopathological Examination

To assess the degree of internal corneal injury, a histopathological analysis of pH-Triggered in Situ Gel Containing Nanoparticles was performed. The cornea utilised in the ex-vivo permeation investigation was employed for the investigation. Following the permeation study, the treated cornea was taken out of the diffusion cell and put in an 8% v/v formalin solution. To create a solid block, the cornea was solidified with paraffin wax after being cleaned of any remaining water with alcohol. A cross-section of the prepared solid block was cut using a microtome cutter and stained with hematoxylin and eosin. Ultimately, a digital Motic microscope (Motic digital Microscope, B3 DMWB, Pal system, Japan) was used to view the slide at a magnification of 40x. The pictures obtained were then compared to a control cornea that had been saline-treated (0.9% NaCl).

Isotonicity Evaluation

The blood sample was subjected to an isotonicity test using pH-Triggered in Situ Gel Containing Nanoparticles and normal saline (0.9% w/v). A drop of blood and a drop of the test sample were completely combined on a glass slide to create the thin film. After letting the film air dry, a drop of Leishman's stain was added to colour it. After a few minutes, the slide was set aside, and extra dye was cleaned off with water. A light microscope set to 40x was used to examine the slide of each treated sample. To check for damage, the red blood cell was examined and compared to normal saline.

Ocular Irritation Study

The Hen's egg chorioallantoic membrane test (HET-CAM) was used for this investigation. The fertilised hen egg was obtained from the nearby chicken house and was kept for ten days at 37˚C and 60% relative humidity in a rotating humidified incubator. The egg was taken out of the incubator on the tenth day, and the CAM was determined using a slit lamp. Using sterile forceps, the eggshell was delicately cracked from the side of the air chamber and the membrane was extracted. The irritation scores were recorded at different intervals (0 minutes, 2 minutes, and 5 minutes) after one drop of pH-Triggered in Situ Gel Containing Nanoparticles, normal saline (0.9 % NaCl, negative control), and sodium hydroxide (0.1 M NaOH, positive control) were applied over the CAM. The scoring was completed using the typical scoring methodology displayed in Table 4.

Table 4: Standard HET-CAM Score Used to Evaluate Ocular Tolerance

Sr.no.	Effect of Formulation on CAM	Score	Presumption
1	No visible hemorrhage	0	No irritation
2	Observable membrane discoloration	1	Mild-irritant
3	Structure cover partially the area of CAM due to membrane discoloration	2	Moderate irritant
4	Structure fully covers the area of CAM due to membrane discoloration	3	Severe irritant

Result and Discussion

Optimization

Carteolol -CHNPs were synthesized and optimized with two layers of Box-Behnken design and three variables. With the five-center point, a total of 17 formulation runs were displayed in the design. Particle size (Y1) and entrapment efficiency (Y2) were the dependent variables on which the effects of independent variables [chitosan (A), tripolyphosphate (B), stirring speed (C)] were assessed. Table 1 presents the actual and projected values together with the composition. To find the best fit model, the data from each experimental run was fitted into a different model, such as a linear, first, quadratic, or cubic model. The quadratic model proved to be the best fit, and Table 5 displays the values for both replies.

Table 5: Analysis of Variance Data of Each Response for Formulation (Carteolol -CHTNPs)

Model	Source	Response-1 (Particle Size, Y1)	Response-2 (Entrapment Efficiency, Y2)
Quadratic	Sum of squares	37,705.94	2111.96
	df	9	9
	Mean square	4178.45	224.56
	F-value	8529.61	5275.72
	P-value, Prob>F	< 0.0001	< 0.0001
	Remark	Suggested, significant	
Lack of Fit			
Quadratic	Sum of squares	0.8495	0.06
	df	3	3
	Mean square	0.29	0.018
	F-value	0.48	0.29
	P-value, Prob>F	0.74	0.85
	Remark	Suggested, nonsignificant	
Residual			
Quadratic	Sum of squares	3.36	0.32
	df	7	7
	Mean square	0.49	0.05

For both responses, the quadratic model's lack of fit value was determined to be nonsignificant (P>0.05). It was found that there was minimal percent variance between the observed and projected values, indicating that the model was well fitted. Analysis of variance was used to examine the greater regression coefficient value (around 1) and Fisher (F) value compared to other models (ANOVA). Software was used to assess the statistical regression and ANOVA of the best-fit model. The results are shown in Table 6.

Table 6: Statistical Summary Used Design for the Formulation (Carteolol -CHTNPs)

Response-1 (Particle Size, Y1)					
Source					
Linear	0.847	0.811	0.701	20.78	-
2FI	0.873	0.797	0.436	21.56	-
Quadratic	0.999	0.999	0.999	0.69	Suggested
Response-2 (Particle size, Y2)					
Linear	0.884	0.857	0.759	4.23	-
2FI	0.988	0.982	0.951	1.49	-
Quadratic	0.999	0.999	0.999	0.21	Suggested

The software produced the polynomial equation for the quadratic model of both responses, demonstrating a notable impact on each response. The influence of each variable, both alone and in combination, on the particle size and encapsulation efficiency has been demonstrated. For every response, a three-dimensional plot and a contour plot were produced, which clarified the interaction impact between the independent variables (Figure 1A and B). It was discovered that both replies' appropriate precision quadratic models were larger than four, indicating that the model was well-fitted.

A.

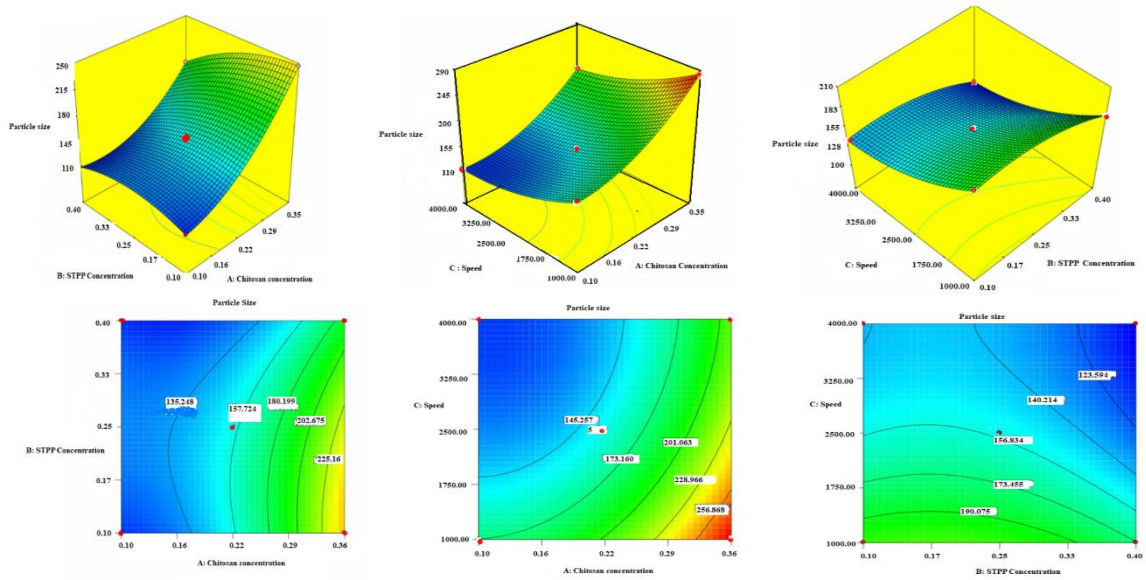

B.

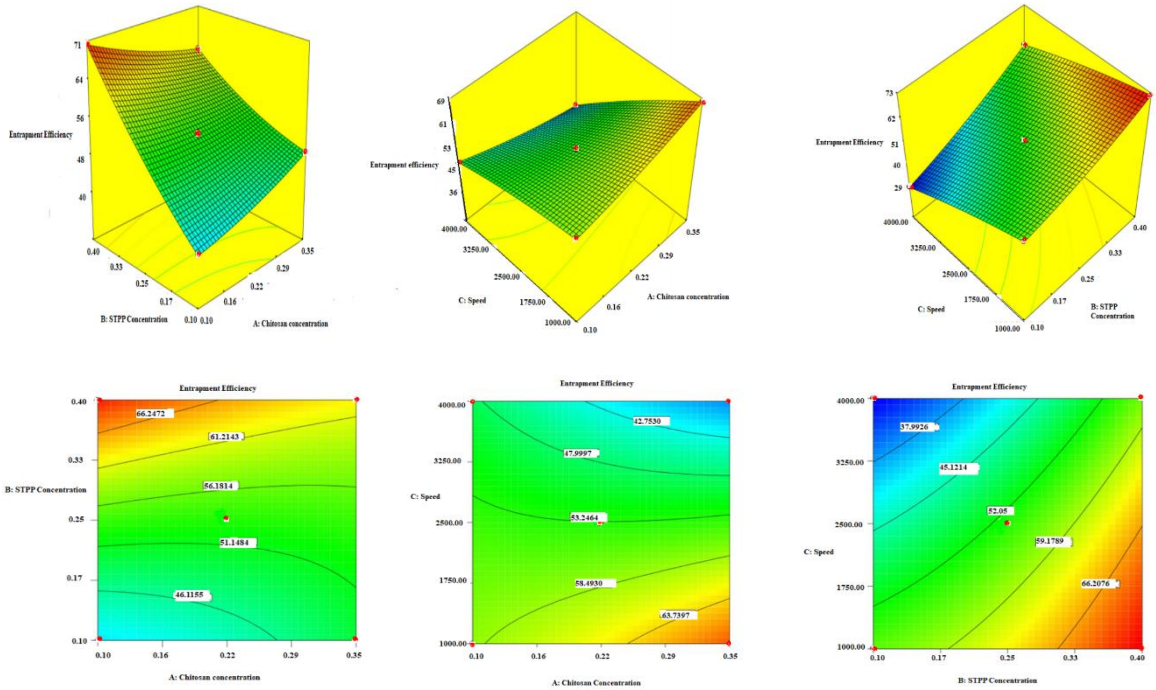

Figure 1: (A) 3D response surface plot and contour plot showing the effect of independent variables on particle size (X1). (B) 3D response surface plot and contour plot showing the effect of independent variables on entrapment efficiency (X2)

Effect of Formulation Variable on Particle Size (Y1)

All 17 formulations were found to have particle sizes between 103.3 nm (F12) and 284.8 nm (F6). The expression of the 3D and contour plot (Figure 1A) was used to assess the separate and aggregate effects of the formulation variable. The model is significant ($P<0.05$), as indicated by the model F-value of 8630.7. Particle size is directly influenced by the significant ($P<0.05$) model terms A, B, C, AB, AC, BC, A2, B2, and C2. The formulation model fared well because the lack of fit was determined to be nonsignificant

(P>0.05) (Table 5). For response 1 (Y1), the quadratic model's second order polynomial equation is as follows:

Particle size (Y1) = +155.12+51.82 A-16.40 B-33.70 C- 15.74 AB-5.90 AC-0.87 BC+27.04 A2 -15.46 B2 +16.25 C2

Where AB, AC, and BC are an independent variable's interaction terms and A, B, and C are its independent variables. The positive and negative indicators stand for the effects that have an impact on the response, respectively. According to the polynomial equation, a rise in CH (A) concentration was accompanied by an increase in particle size. A rise in the viscosity of the CH solution is the cause of the particle size increase. With STPP, the conductivity drops and there isn't any full intra- and intermolecular crosslinking. Particle size was shown to be antagonistically affected by STPP (B), with smaller particles resulting from higher STPP concentrations. Higher crosslinking occurs between NH3 + (CH) and PO4 − (STPP). Due to the presence of more PO4 - of STPP on the surface of NPs than NH3 +, there is a drop in surface charge and an increase in particle size at high concentrations of STPP. Particle size was more adversely affected and more noticeably so by the stirring speed (C). Particle size reduced with increased swirling speed (C). It hastens the breakdown of NPs by increasing the shear force caused by the mixing of STPP dispersion into the CH solution. In contrast, the combined impact of STPP and CH (A and B) demonstrated a more pronounced negative influence on particle size than did the combined effects of STPP and stirring speed (BC) and CH (AC). Particle size reduces as CH and STPP concentrations rise at the same time. The intermolecular and intramolecular gelation between NH3 + /PO4− is more intricate.

When the proposed formulation was tested against another kinetic model, the quadratic model fit the data the best, with an R2 that was nearly unity when compared to the other model (Table 6). With an adjusted R2 of 0.998 showing that the model has a strong signal, the expected R2 of 0.998 is in reasonable agreement with the sufficient precision of 336.26 (>4).

Effect of Formulation Variable on Entrapment Efficiency (Y2)

As indicated in Table 1, the developed formulation displayed the percentage of EE in the range of 31.2% (F11) to 71.34 % (F3). The proximity of the actual and anticipated values indicates the closeness of the outcome data. The 3D and contour plot (Figure 1B) are used to evaluate the contribution of each formulation variable alone and in combination. For the formulation model, the nonsignificant value (P>0.05) provided by the lack of fit is good (Table 5). Figure 1B and the polynomial equation were utilised to interpret how formulation factors affected entrapment efficiency (Y2):

Entrapment efficiency (Y2) = +53.32–4.057A+11.82B- 11.28C-5.29AB−6.48AC+3.09BC+0.98A2 +2.83 B2 -2.02C2

where AB, AC, and BC are combined variables and A, B, and C are independent variables (STPP, CH, and stirring speed). The synergistic and antagonistic effects of the variables on the response were expressed using the positive and negative signs. The polynomial equation demonstrated that stirring speed (C) and STPP (B) have a greater impact than CH (A). The entrapment effectiveness was shown to decrease with increasing CH content (A) because of the viscosity of CH. Low drug entrapment results from reduced interaction between CH and STPP (NH3 + /PO4 −) at high viscosity. When the protonated ion of CH (NH3 +) gels at a higher phosphate ion concentration, a large amount of medicine diffuses in NPs during crosslinking. While less pronounced than STPP, the stirring speed has a detrimental impact on EE. Shear force increases with increasing stirring speed, leading to the breakdown of nanoparticles and drug leaching from the polymer matrix, ultimately resulting in a drop in EE.

The quadratic model was found to have the highest F-value and regression coefficient (R2) when compared to the linear, first-order, and cubic models, as determined by the ANOVA calculation. This suggests that the quadratic model is the best-fit and is statistically significant (P<0.0001). The corrected R2 (0.998) and the projected R2 (0.998) agree rationally (Table 4). A nonsignificant (P<0.05) lack of fit was discovered, and there was less fluctuation between the response's actual and projected values. When the precision is higher than 4 (265.7), the model's signal is deemed sufficient.

Point Prediction Optimization

To determine the ideal composition of optimised NPs, point prediction optimisation was used (Carteolol CHNP opt). The optimal combination of low size and high EE was demonstrated by the optimised composition CH (0.22% w/v), STPP (0.25% w/v), and stirring speed (2500 rpm). The composition revealed an entrapment effectiveness of 54.06 ± 4.33% and an actual particle size of 153 ± 6 nm. The software yielded the expected values for particle size and encapsulation efficiency, which were 155.12 nm and 53.32 percent, respectively. The actual outcome was discovered to be extremely like the anticipated outcome. For particle size, the percent error between observed and anticipated values was found to be −2.17%, while for entrapment efficiency, it was found to be +2.42%. Figure 2 shows the outcome of the actual and anticipated values for the entrapment efficiency and particle size.

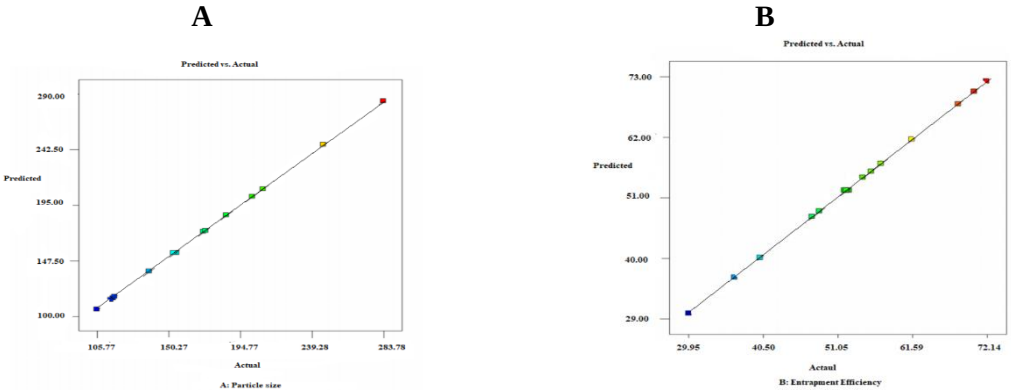

Figure 2: Actual and predicted response of independent variables on (A) particle Size (nm), (B) Entrapment Efficiency (%)

Particle Characterization

Carteolol CHNP opt was determined to have a particle size of 153 ± 6 nm, a PDI of 0.126 ± 0.03, and a zeta potential of +36.25 mV. It was discovered that the particle size fell inside the permitted size range. Particles larger than 1 µm have the potential to irritate eyes. The low PDI value demonstrated a uniform particle distribution and shows that the dispersion of NPs is both stable and nonaggregate. The disaggregated formulation was stable, as shown by the positive zeta potential value of +36.25 mV. The presence of chitosan at the produced formulations' exterior contact is shown by the positive sign of NPs. Figure 3 shows the TEM image, and the electron microscope image verified the creation of uniformly distributed spherical particles.

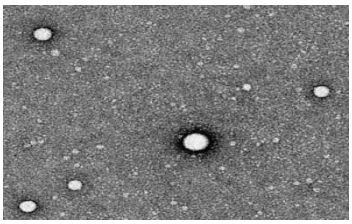

Figure 3: TEM image of optimized Carteolol nanoparticle (Carteolol -CHNP opt)

Thermal Evaluation

The purpose of the DSC investigation was to examine the polymorphic transition of the medication Carteolol following its encapsulation into NPs. Carteolol, CH, and Carteolol -CHNP opt were used in the investigation; Figures 4 A–C display their thermograms. Carteolol thermogram demonstrated a high, recognisable endothermic peak at its melting point of 275˚C, indicating that it is crystalline (Figure 4A). CH displayed two distinct peaks: an exothermic peak at 270°C resulting from degradation and an endothermic broad peak at 73.4 ºC caused by water molecule evaporation (Figure 4B). The thermogram of Carteolol CHNP opt did not show any distinctive Carteolol peak. Figure 4C only showed the peaks at 63.5˚C and 265˚C, indicating that either the drug was present in the NPs matrix in molecular dispersion form or that there had been a loss of crystallinity.

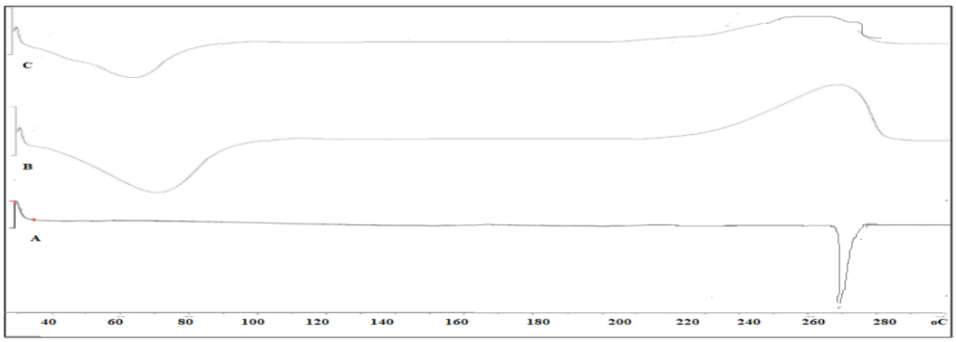

Figure 4: DSC thermogram of (A) Carteolol, (B) chitosan, (C) optimized Carteolol nanoparticles (Carteolol -CHNP opt)

X-Ray Diffraction Study

The purpose of the study was to assess each tested sample's atomic-level crystal lattice configuration. The diffraction patterns of Carteolol, CH, and Carteolol -CHNP opt are shown in Figures 5 A–C. Carteolol crystalline nature was confirmed by the intense distinctive peak it displayed at diffraction angles of 2θ, 11.3, 14,28, 16.96, 20.11, 20.24, 23.14, 23.25, and 26º. On the other hand, CH displayed a noticeable broad diffraction peak at 10.5º and 21º at 2θ angle. Even though the chitosan was developed in an aqueous medium, the solitary crystal lacked water. The high temperature of crystal formation provides an explanation. A Carteolol-CHNP opt diffractogram did not show a distinctive Carteolol diffraction peak. This finding suggested that the crystalline to amorphous form transition and subsequent structural changes may be the cause of the shift in the characteristic diffraction peak. Carteolol is entirely dissolved and enmeshed in the TPP and chitosan polymer.

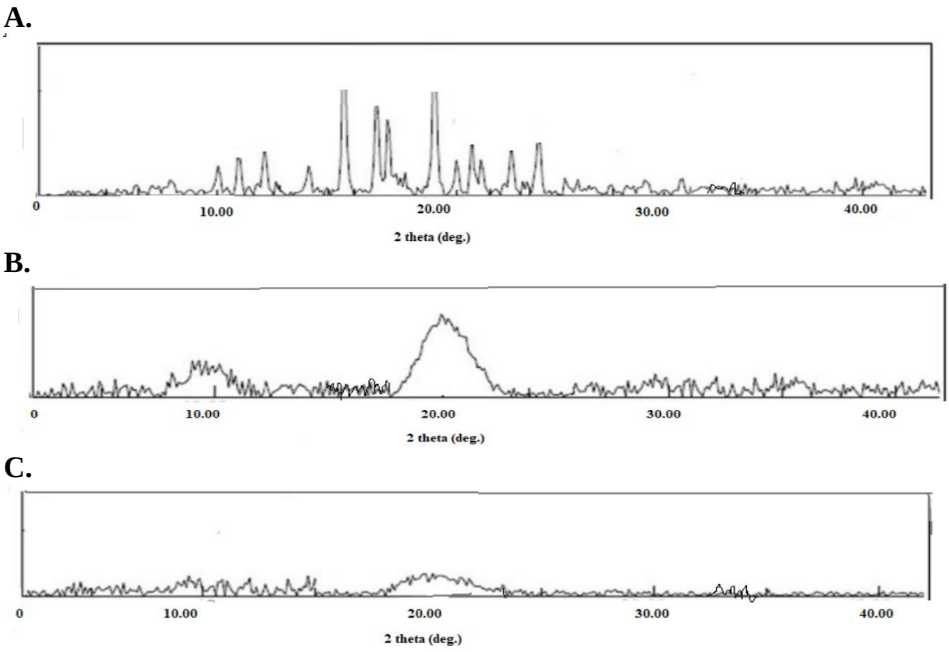

Figure 5: XRD image of (A) Carteolol, (B) chitosan, (C) optimized Carteolol nanoparticles (CTM-CHNP opt)

In-vitro Release Study

Figure 6 shows the results of the in-vitro release studies for Carteolol-CHNP opt and Carteolol-solution. With the Carteolol-CHNP opt, a dual release pattern was seen: first, a rapid burst release (26.9 ± 3.4% in 1 hour), followed by a steady, continuous release (83.8 ± 4.8% in 12 hours). In three hours, the drug release from Carteolol -solution was approximately 98.8 ± 5.8%, while the drug release from Carteolol -CHNP opt was 39.7 ± 4.8. Carteolol was discovered to have leaked from the surface of NPs, causing the first burst release. The slower drug diffusion from the polymer core allowed for a prolonged and gradual release of

Carteolol. A differential kinetic model was fitted to the Carteolol -CHNP opt formulation release data. Korsmeyer-Peppas model (r2 = 0.997) >first order (r2 = 0.996) >Higuchi (r2 = 0.994) >Hixon–Crowell model (r2 = 0.990) >zero-order (r2 = 0.953) is the order of regression coefficient. The Korsmeyer-Peppas model had the greatest regression coefficient and was recommended as the model with the best fit. The Korsmeyer Peppas model's release exponent is ≤0.5 (0.475), indicating that Fickian diffusion governs the drug release process and that the molecular diffusion CHNPs system determines the rate of carteolol release into the release medium.

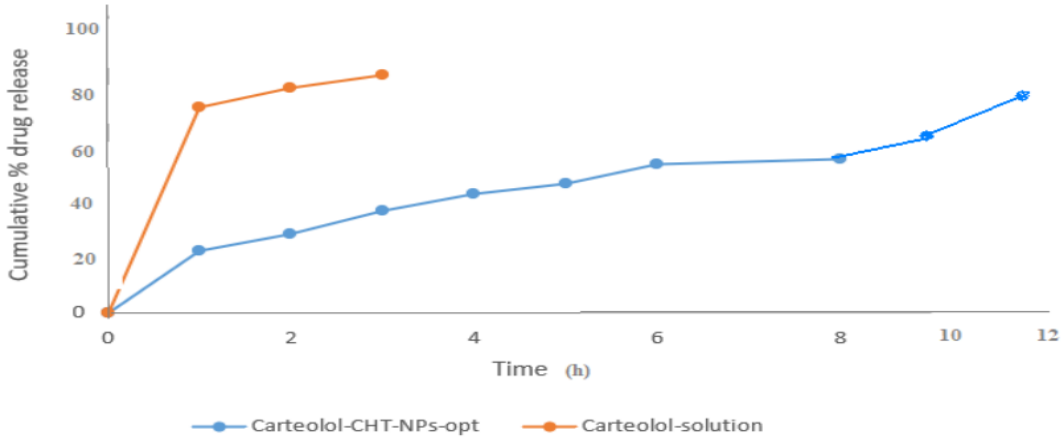

Figure 6: Comparative drug release profile of optimized Carteolol nanoparticles (Carteolol-CHNP opt) and Carteolol solution. Values are presented as mean ± SD with triplicates

FORMULATION OF NANOPARTICLE LOADED THERMOSENSITIVE *IN SITU* GEL

Characterization of nanoparticles loaded in situ gel

Clarity and Ph

Table 7: Clarity and pH of *in situ* gel

Batch Name	pH	Clarity
F1	6.4	Clear
F2	6.8	Clear
F3	6.5	Clear

Gelling Capacity

Table 8: Gelling capacity of prepared *in situ* gel

Batch Name	Gelling capacity
F1	+++
F2	++
F3	++

Viscosity

Table 9: Viscosity of prepared NPs loaded *in situ* gel before and after gelation

Batch Name	Viscosity at 20 rpm before gel formulation (cPs)	Viscosity at 20 rpm after gel formulation (cPs)
F1	4521	7683
F2	5823	8630
F3	5967	8924

Drug Release

Table 10: Percent cumulative drug release from NPs loaded *in situ* gel

Time (hr)	% CDR		
	F1	F2	F3
0	0	0	0
1	15.62	14.62	16.82
2	21.87	19.09	20.78
3	29.74	22.76	25.65
4	34.26	31.78	31.82

5	42.92	39.93	38.56
6	46.31	47.64	42.90
7	50.32	51.56	47.54
8	54.32	56.32	53.53
9	57.51	59.54	62.76
10	61.82	65.67	69.45

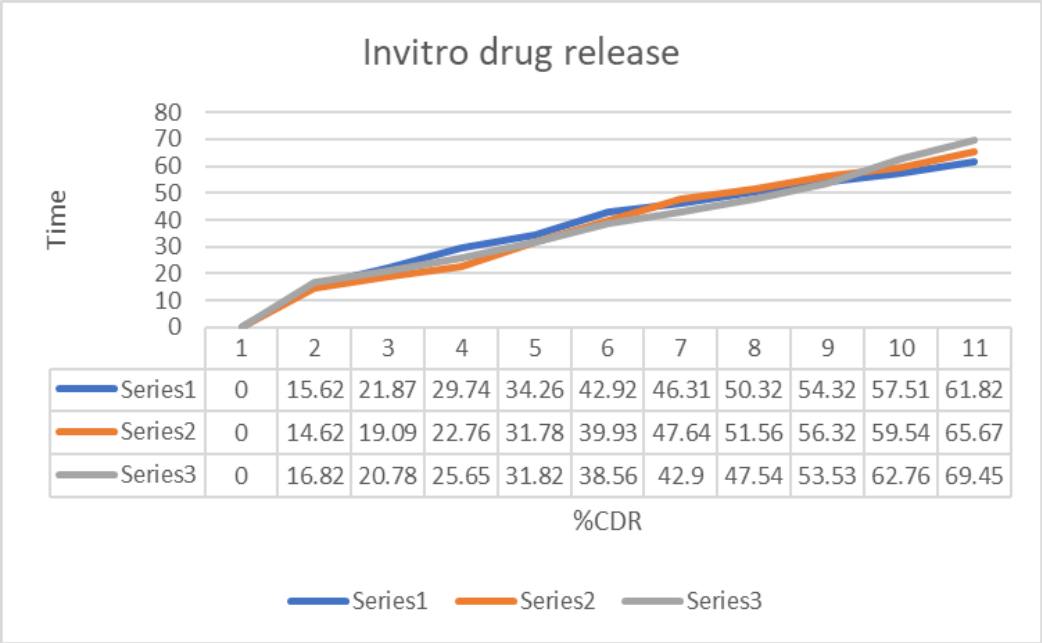

Figure 7: Percentage drug release from nanoparticle loaded in situ gel (F1-F3)

Gelation Temperature

Table 11: Gelation temperature of NPs loaded in situ gel

Batch Name	Gelation temperature (˚C)
F1	38.52±0.21
F2	37.87±0.10
F3	37.78±0.26

Prepared all batches showed gelation at temperature in the range 37.78 ± 0.26 ˚C to 38.52 ± 0.21 ˚C. Formulation must possess gelation temperature at or near to physiological temperature. If it is very high then it may fail to gel at body temperature and if it is too less, then it may create some administration related issues. Therefore; batch F3 was selected as optimized batch which showed gelation at temperature 37.78 ± 0.26 ˚C.

Sterility Testing

a. Sterility testing by using soyabeancasein digest medium (*C. albicans*)
b) Sterility testing by using alternate thioglycolate medium (*S. aureus*)

Figure 8: Sterility testing

FORMULATION OF pH-TRIGGERED IN SITU GEL CONTAINING NANOPARTICLES

Table 12: Formulation Contents of pH-Triggered in Situ Gel Containing Nanoparticles

Ingredient	F1	F2
Carteolol nanoparticles	0.25	0.25
Carbopol	0.5	0.5
Methocel E50 LV	1.5	1.5
Sodium hydroxide	0.16	0.16
Benzalkonium chloride	0.02	0.02
Tween 20	-	1.0
Citric acid	0.407	0.407
Disodium hydrogen phosphate	1.125	1.125
Purified water	100ml	100ml

Evaluation of formulations

Clarity by visual observation against a black and white background in a well-lit cabinet, pH.

Table 13: Evaluation of formulations

Formulation	Drug content (% w/v)	pH	Clarity
F1	98.52	6.03	Clear
F2	99.26	6.03	Clear

In-vitro release studies

Table 14: In-vitro drug release of pH.-triggered in situ gel containing nanoparticles

Time	% CDR	
	F1	F2
0	0	0
1	23.67	28.37
2	32.98	36.98
3	45.78	48.37
4	57.45	60.03
5	66.65	71.46
6	75.36	80.56
7	81.87	84.16
8	86.89	89.96
9	91.14	94.37
10	98.52	99.26

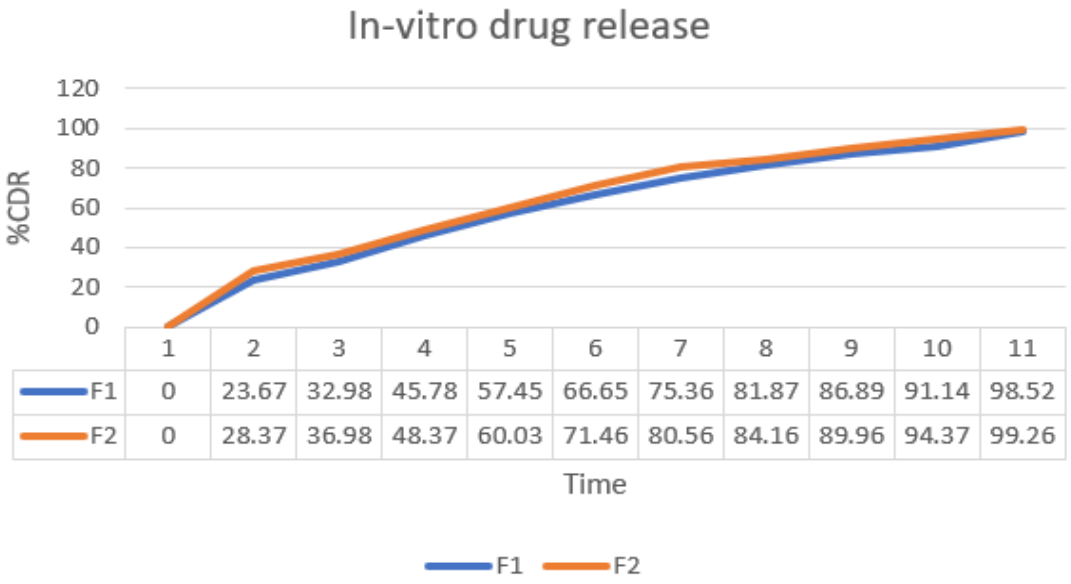

Figure 9: In-vitro drug release of pH-triggered in situ gel containing nanoparticles

Permeation Study

Results of an ex-vivo investigation on corneal permeation using pH Triggered in Situ Gel Containing Nanoparticles and Carteolol-solution were presented in Figure 10. A noteworthy variation in penetration was noted. Compared to Carteolol-solution (72.57 µg/cm2, 29.63%), the pH-Triggered in Situ Gel Containing Nanoparticles sample demonstrated a considerable ($P<0.05$) increased penetration of 195.22 µg/cm2 (78.64%). pH-Triggered in Situ Gel Containing Nanoparticles showed a 2.72-fold increase in permeability compared to the Carteolol-solution. Additionally, the flow for pH-Triggered in Situ Gel Containing Nanoparticles and Carteolol-solution was estimated; the results revealed, respectively, 31.94 µg/cm2 /h and 12.84 µg/cm2 /h. The presence of CH as a polymer and nanoparticle allowed for greater penetration and flux. In addition to possessing the cationic charge on NPs, it also has the bioadhesive and permeation-enhancing properties. Precorneal residence duration and penetration are increased when the anionic charge of corneal mucin and the cationic charge of CH combine. The mucoadhesive property of CH led to a better retention of NPs laden gel at the ocular surface, which in turn allowed for improved drug absorption. The negative charge of corneal mucin interacts ionic with the protonated amino group of CH. Widening of the NPs-loaded gel's endocytic absorption increased the drug's transport along the paracellular pathway once it was released.

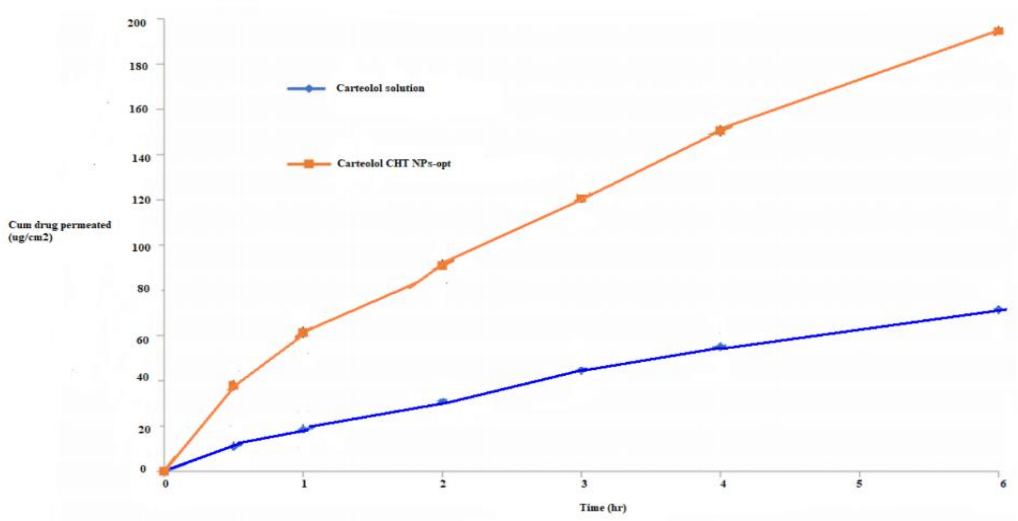

Figure 10: Comparative drug permeation profile of optimized pH-Triggered in Situ Gel Containing Nanoparticles and Carteolol solution. Values are presented as mean ± SD with triplicates

Bioadhesion Study

An investigation into the bioadhesion of the pH-Triggered in Situ Gel Containing Nanoparticles formulation was conducted, and the outcome demonstrated superior bioadhesion characteristics, measuring 90.87 ± 3.7%. The mucoadhesive properties of CH and its positive zeta potential value account for the high bioadhesion. Mucoadhesion is significantly influenced by the positive value of zeta potential, which indicates the positive surface of the gel loaded with NPs. The negatively charged mucin sialic group can readily interact with the positively charged chitosan NPs loaded pH-Triggered in Situ Gel. A stable NPs-loaded gel is formed as a result of their increased contact, and this could be a sign of a potential delivery mechanism. This finding suggests that corneal mucin will bind to CHNPs loaded pH-Triggered in Situ gel.

Corneal Hydration Study

The hydration test can be used to assess the damage to the eyes. The cornea subjected to pH-Triggered in Situ Gel Containing Nanoparticles exhibited a notable degree of hydration; the result fell within the permissible range of 77–81 percent (i.e., 80.05 ± 1.79 percent). This result indicated that the pH-Triggered in Situ Gel Containing Nanoparticles did not damage the ocular tissue (epithelium or endothelium) and had an acceptable hydration limit. The cornea's histological analysis provided additional confirmation of the outcome.

Histopathological Examination

To assess the internal damage to the cornea following treatment with pH-Triggered in Situ Gel Containing Nanoparticles, a histopathology investigation was conducted. The sodium chloride (0.9 % NaCl, control) and

the treated cornea with pH-Triggered in Situ Gel Containing Nanoparticles were contrasted (figure not shown). No changes to the cornea's morphology or histology were noticed. Similar to the sample treated as a control, the cornea's stroma, Bowman's membrane, and epithelium were all confirmed to be intact. Additionally, the cornea's morphology was kept in good condition. The investigation verified that the in-situ gel containing CHNPs is safe and non-toxic for use in ocular applications. According to the findings of the histopathology investigation, pH Triggered in Situ Gel Containing Nanoparticles can be used safely.

Isotonicity Evaluation

The pH-Triggered in Situ Gel Containing Nanoparticles and blood compatibility was assessed using the isotonicity evaluation. The isotonicity between normal saline (control) and pH-Triggered in Situ Gel Containing Nanoparticles is assessed in Figures 11A and B. After being incubated with erythrocytes, pH-Triggered in Situ Gel Containing Nanoparticles showed minimal homolysis and RBC cell injury (Figure 11 A). The outcome was discovered to be like the blood treated with regular saline (Figure 11 B). This demonstrated the hemocompatibility and safety of pH-Triggered in Situ Gel Containing Nanoparticles for usage in future in vivo applications.

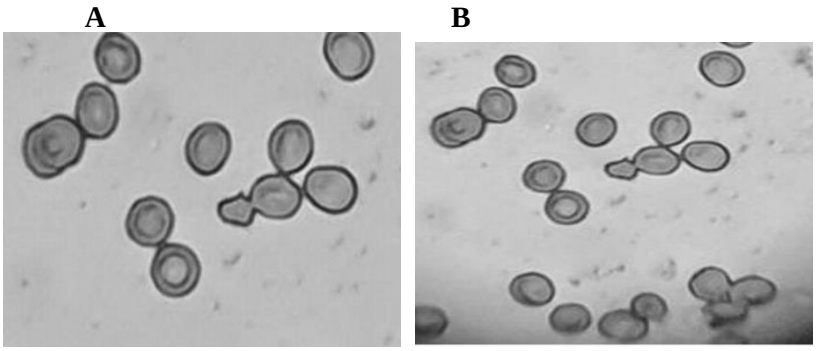

Figure 11: Comparative isotonicity image (A) pH-Triggered in Situ Gel Containing Nanoparticles, (B) normal saline (control)

Ocular Irritation

The pH Triggered in Situ Gel Containing Nanoparticles, normal saline (negative control), and 0.1 M NaOH (positive control) treated fertilized hen egg were tested in order to verify the results of the ocular tolerance research. The photographs in Figure 26 were used as the basis for scoring, which followed the standard scale displayed in Table 4. After five minutes of therapy, the pH-Triggered in Situ Gel Containing Nanoparticles and the normal saline-treated group displayed a mean score of zero, whereas the 0.1 NaOH (positive control) treated group displayed a mean score of 15.5. The groups treated with normal saline (negative control) and pH Triggered in Situ Gel Containing Nanoparticles did not exhibit any blood vessel damage or rupture (non-irritant). The positive control-treated group showed notable blood vessel damage and was classified as an irritating group. Based on the findings, we deduced that the created nano-formulation is safe to provide topically.

Conclusion

Chitosan nanoparticles loaded with carteolol (Carteolol-CHNPs) were synthesised via ionotropic gelation. The box-Behnken design was used to improve the formulation using variables including CH (A), STPP concentration (B), and stirring speed (C). They created its in-situ gel and evaluated how it affected the independent variables, like entrapment efficiency (Y2) and particle size (Y1). Carteolol-CHNP opt claims that the particle size is less than 200 nm, making it ideal for ocular administration. The generated formulation's positive zeta potential shows that the particles are spherical and not aggregated. The thermal and x-ray diffraction investigations demonstrated that Carteolol was dispersed uniformly throughout the polymer matrix. A sustained release profile with significantly better corneal permeability ($P<0.05$) was obtained in comparison to Carteolol-solution. The results of the HET-CAM test, histology, and hydration tests revealed that the excised goat cornea did not exhibit any evidence of visual impairment. The outcomes shown that glaucoma patients with a longer precorneal residency length and better patient compliance could benefit from the use of Carteolol-CHNPs loaded in-situ gel by reducing the dosage frequency.

References

1. Hasan A. Design and *in vitro* characterization of small unilamellar niosomes as ophthalmic carrier of dorzolamide hydrochloride. Pharm Dev Technol. 2014; 19(6): 748-754.
2. Hoyng P., Van Beek L. Pharmaceutical therapy for glaucoma : a review. Drugs. 2000; 59:411-34.
3. Sasaki H., Yamamura K., Nishida K., Nakamura J., Ichikawa M. Delivery of drugs to the eye by topical application. Prog Retin Eye Res. 1996;15: 583-620.
4. Kumar R, Sinha V. Preparation and optimization of voriconazole microemulsion for ocular delivery. Colloids Surf B. 2014; 117: 82-88.
5. Davies N. Biopharmaceutical considerations in topical ocular drug delivery. Clin Exp Pharmacol Physiol. 2000; 27:558-562.
6. Nanjawade B., Manvi F., Manjappa A. *In situ*-forming hydrogels for sustained ophthalmic drug delivery. J Control Release. 2007;122:119-34.
7. Almeida H., Amaral M., Lobao P., Lobo J. *In situ* gelling systems : a strategy to improve the bioavailability of ophthalmic pharmaceutical formulations. Drug Discov Today. 2014;19:400-412.
8. Meisner D., Mezei M. Liposome ocular delivery systems. Adv Drug Delivery Rev. 1995;16:75-93.
9. Shrividya B., Cardoza R., Amin P. Sustained ophthalmic delivery of ofloxacin from a pH triggered *in situ* gelling system. Journal control Release. 2001;73:205-211.
10. Al-Tahami K., Singh J. Smart polymer-based delivery systems for peptides and proteins. Recent Pat Drug Deliv Formul. 2007;1:65-71.
11. Cantor L. Brimonidine in the treatment of glaucoma and ocular hypertension. Ther Clin Risk Manag. 2006:2(4): 337-346.
12. Miyazaki S., Suzuki S., Kawasaki N., Endo K., Takahasi A., Attwood D. *In situ* gelling xyloglucan formulations for sustained release ocular delivery of pilocarpine hydrochloride. Int J Pharm. 2001; 229:29-36.
13. You J., Almeda D., Ye G., Auguste D. Bio responsive matrices in drug delivery. J Biol Eng. 2010; 4:1-12.
14. Hartmann V., Keipert S. Physicochemical, *in vitro* and *in vivo* characterization of polymers for ocular use. Pharmazie. 2000;55:440-443.
15. Lee C. Moturi V., Lee Y. Thixotropic property in pharmaceutical formulations. J Control Release. 2009;136:88-98.
16. Pisal P., Patil S., Pokharkar V. Rheological investigation and its correlation with permeability coefficient of drug loaded carbopol gel: influence of absorption enhancers. Drug Dev Ind Pharm. 2013; 39: 593-599.
17. Tamburic S., Craig D. Rheological evaluation of polyacrylic acid hydrogels. J Pharm Sci. 1995;1:107-109.
18. Ameeduzzafar SS., Abbas Bukhari SN., Ahmad J., Ali A., Ali A. Formulation and optimization of levofloxacin loaded chitosan nanoparticle for ocular delivery: in-vitro characterization, ocular tolerance and antibacterial activity. *Int J Biol Macromol*. 2018;108:650–659.
19. Paliwal R., Paliwal SR., Sulakhiya K., Kurmi BD., Kenwat R., Mamgain A. Chitosan-based nanocarriers for ophthalmic applications. *Polysaccharide Carriers Drug Deliv*. 2019;79–104.
20. Chrisp P., and Sokin E. M. Ocular carteolol. A review of its pharmacological properties, and therapeutic use in glaucoma and ocular hypertension. Drug Aging. 1992; 2:58–77.
21. MRP Rao, S Taktode, SS Shivpuje, S Jagtap. Optimization of Transmucosal Buccal Delivery of Losartan Potassium using Factorial Design. Indian Journal of Pharmaceutical Education and Research, 2016; 50(2): S132-S139.
22. N Patre, S Patwekar, S Dhage, S Shivpuje. Formulation & Evaluation Of Piroxicam Bionanocomposite For Enhancement of Bioavailability. European Journal of Molecular & Clinical Medicine, 2020; 7(11): 9362-9376.
23. SJ Wadher, SL Patwekar, SS Shivpuje, SS Khandre, SS Lamture. Stability Indicating Assay Methods for Simultaneous Estimation of Amoxicillin Trihydrate And Cloxacillin Sodium in Combined Capsule Dosage Form by UV-Spectrophotometric Method. European Journal of Biomedical and Pharmaceutical sciences, 2017; 4(10): 858-864.
24. Santosh A. Payghan Shivraj S. Shivpuje Shailesh L. Patwekar, Karna B. Khavane, Padmavati R. Chainpure. A Review on Different Preparation Method Used For Development of Curcumin Nanoparticles. International Journal of Creative Research Thoughts, 2021;9(1):4088-4101.

25. Zeba Ashfaq Sheikh P. R. Chainpure, S. L. Patwekar, S. S. Shivpuje. Formulation and evaluation of Garciniacambogia and Commiphoramukul Herbal tablets used for AntiObesity. International Journal of Engineering, Science and Mathematics, 2019; 8(4): 180-195.
26. Pravin P Karle, Shashikant C Dhawale, Vijay V Navghare, Shivraj S Shivpuje. Optimization of extraction conditions and evaluation of Manilkara zapota (L.) P. Royen fruit peel extract for in vitro α-glucosidase enzyme inhibition and free radical scavenging potential. Future Journal of Pharmaceutical Sciences, 2021; 7(1):1-10.
27. Sheetal Rathod P. R. Chainpure, S. L. Patwekar, S. S. Shivpuje. A Study Of Carica Papaya Concerning It's Ancient And Traditional Uses - Recent Advances And Modern Applications For Improving The Milk Secretion In Lactating Womens. International Journal of Research, 2019;8(2):1851-1861.
28. Shivraj S. Shivpuje Shailesh J. Wadher, Bhagwan B. Supekar. Development And Validation Of New Ft-Ir Spectrophotometric Method For Simultaneous Estimation Of Ambroxol Hydrochloride And Cetirizine Hydrochloride In Combined Pharmaceutical. International Research Journal of Pharmacy, 2019; 10(3):110-114.
29. Shivraj S. Shivpuje, Shailesh J. Wadher, Bhagwan B. Supekar. Simultaneous Estimation of Ambroxol Hydrochloride and Cetirizine Hydrochloride in Combined Solid Tablet Formulations by HPTLC-Densitometric Method. Asian Journal of Biochemical and Pharmaceutical Research, 2019; 9(1):1-10.
30. JW Sailesh, SS Shivraj, SI Liyakat. Development and Validation of Stability Indicating RP-HPLC Method for the Estimation of Simvastatin in Bulk and Tablet Dosage form. Research Journal of Pharmacy and Technology, 2018; 11(4): 1553-1558.
31. Patil S. S. Shivpuje Shivraj S. Patre Narendra G. Development and Validation Of Stability Indicating HPTLC Method For Determination of Nisoldipine (Niso) In Tablet Dosage Form. European Journal of Biomedical and Pharmaceutical sciences, 2017; 4(12):462468.
32. W Shailesh, K Tukaram, S Shivraj, L Sima, K Supriya. Development and Validation of Stability Indicating UV Spectrophotometric Method for Simultaneous Estimation of Amoxicillin Trihydrate and Metronidazole In Bulk And In-House Tablet. World Journal of Pharmaceutical and Medical Research, 2017;3(8):312-318.
33. J Wadher Shailesh, M Kalyankar Tukaram, S Shivpuje Shivraj. Development and Validation of Stability Indicating Assay Method for Simultaneous Estimation of Amoxicillin Trihydrate and Cloxacillin Sodium In Pharmaceutical Dosage Form By Using RP-HPLC. World Journal of Pharmaceutical Research, 2017; 10(6):1002-1006.
34. Shital S. Sangale, Priyanka S. Kale, Rachana B. Lamkane, Ganga S. Gore, Priyanka B. Parekar, Shivraj S. Shivpuje (2023). Synthesis of Novel Isoxazole Derivatives as Analgesic Agents by Using Eddy's Hot Plate Method. South Asian Res J Pharm Sci, 5(1): 18-27.
35. Priyanka B. Parekar, Shivraj S. Shivpuje, Vijay V. Navghare, Manasi M. Savale, Vijaya B. Surwase, Priti S. Mane- Kolpe, Priyanak S. Kale. Polyherbal Gel Development And Evaluation For Antifungal Activity, European Journal of Molecular & Clinical Medicine. 2022; 9(03): 5409-5418.
36. Jain AA, Mane-Kolpe PD, Parekar PB, Todkari AV, Sul KT, Shivpuje SS. Brief review on Total Quality Management in Pharmaceutical Industries, International Journal of Pharmaceutical Research and Applications. 2022; 7(05):1030-1036.
37. Sumaiyya. K. Attar, Pooja P. Dhanawade, Sonali S. Gurav , Prerna H. Sidwadkar , Priyanka B. Parekar, Shivraj S. Shivpuje. Development and Validation of UV Visible Spectrophotometric Method for Estimation of Fexofenadine Hydrochloride in Bulk and Formulation, GIS SCIENCE JOURNAL. 2022; 9(11): 936-944.
38. Sumayya Kasim Atar, Priyadarshini Ravindra Kamble, Sonali Sharad Gurav, Pooja Pandit Dhanawade, Priyanka Bhanudas Parekar, Shivraj Sangapa Shivpuje. Phytochemical Screening, Physicochemical Analysis of Starch from Colocasia Esculenta, NeuroQuantology, 2022; 20(20): 903-917.
39. Priti D.Mane-Kolpe, Alfa A. Jain, Tai P. Yele, Reshma B. Devkate, Priyanka B. Parekar, Komal T. Sul, Shivraj S. Shivpuje. A Systematic Review on Effects of Chloroquine as a Antiviral against Covid-19, International Journal of Innovative Science and Research Technology, 2022;7(11): 989-995.
40. Dr. Rohit Jadhav, Prof. Abhay D. Kale, Dr. Hitesh Vishwanath Shahare, Dr. Ramesh Ingole, Dr Shailesh Patwekar, Dr S J Wadher, Shivraj Shivpuje. Molecular Docking Studies and Synthesis of Novel 3-(3-hydroxypropyl)-(nitrophenyl)[1,3] thiazolo [4,5-d] pyrimidin2(3H)-one as potent inhibitors of P. Aeruginosa of S. Aureus, Eur. Chem. Bull. 2023; 12(12): 505-515.
41. Priyanka B. Parekar, Savita D. Sonwane, Vaibhav N. Dhakane, Rasika N. Tilekar, Neelam S. Bhagdewani, Sachin M. Jadhav, Shivraj S. Shivpuje, Synthesis and Biological Evaluationof Novel 1,3,4-

Oxadiazole Derivatives as Antimicrobial Agents, Journal of Cardiovascular Disease Research, 2023; 14(8):611-624.
42. Kavita R. Mane, Prachi A. Ghadage, Aishwarya S. Shilamkar, Vaishnavi A. Pawar, Sakshi B. Taware, Priyanka B. Parekar, Shivraj S. Shivpuje. Phytochemical Screening, Extraction and In-vivo study of Immunomodulation effect of Withania somnifera, Momordicadioica and Annonasqumosa leaves. Journal of Cardiovascular Disease Research, 2023; 14(9): 231-241.
43. MR Rao, S Shivpuje, R Godbole, C Shirsath. Design and evaluation of sustained release matrix tablets using sintering technique. International Journal of Pharmacy and Pharmaceutical Sciences, 2015; 8(2):115-121.